

Hybridization of Singular Plasmons via Transformation Optics

Sanghyeon Yu^{*†}

Habib Ammari^{*}

Abstract

Surface plasmons of strongly coupled metallic nanoparticles are useful for controlling light at the nanoscale. Here we develop a new physical model for understanding plasmons of the interacting many-particle systems. We combine both the plasmon hybridization and transformation optics approaches so that our model gives a simple and intuitive picture when the particles are close-to-touching. In the proposed approach, the system's plasmon is a combination of the gap-plasmons of each pair of particles. This provides new physical insights into how the spectrum of the plasmons depends on the geometry of the system.

1 Manuscript

Metallic nanostructures have been extensively studied and utilized for sub-wavelength control of light due to their unique ability to support surface plasmons, which are oscillations of electron density on metal-dielectric interfaces [1–5]. Among various structures, a system of interacting nanoparticles is of fundamental importance [5]. When the particles are closely spaced, their plasmons exhibit significant spectral shifts, extreme light confinement, and Fano resonances [4] due to their strong electromagnetic interaction. These phenomena have important applications including optical nanocircuits, single molecule sensing, spectroscopy, and nonlinear optics [1–5]. However, understanding the strong interaction between the particles is quite challenging because plasmons depend on the geometry of the particles in a complicated way. It is important to clarify this intricate relationship for a rational design of plasmonic devices.

The plasmon hybridization model results in a simple and intuitive physical picture for plasmons of interacting particles in a way analogous to molecular orbital theory, providing a general and powerful design principle [5–7]. In this model, the hybridized plasmons are viewed as simple combinations of the individual particle plasmons. However, when the particles become close-to-touching, the picture becomes complicated since a large number of uncoupled plasmons contribute to each hybridized plasmon. Recently, Transformation Optics (TO) has been applied to understand the plasmons of two close-to-touching particles and other geometrically singular structures [8–10]. We also refer to [11–60] for related works on close-to-touching particles. TO reveals the hidden symmetries in singular plasmonic systems, thereby giving a unique physical insight into the origin of broadband light-harvesting. TO also yields analytic or semi-analytic solutions. But TO alone cannot be applied to systems featuring three (or more) particles.

^{*}Department of Mathematics, ETH Zürich, Rämistrasse 101, CH-8092 Zürich, Switzerland.

[†]Correspondence to S.Y. (sanghyeon.yu@sam.math.ethz.ch)

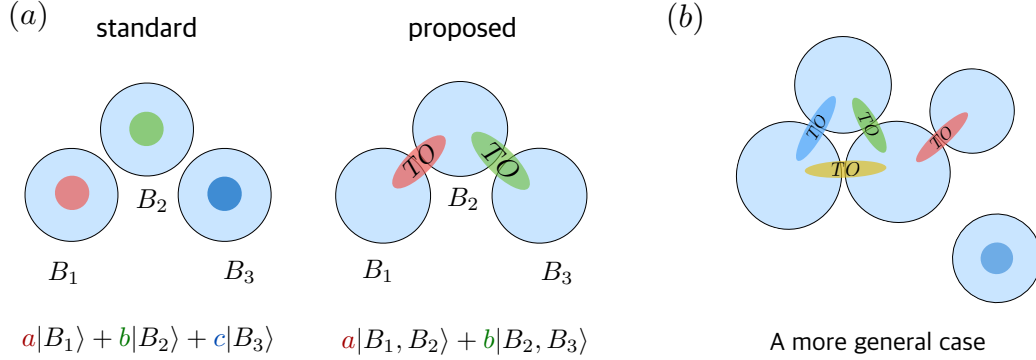


Figure 1: Schematic description of our proposed model. (a) comparison with the standard hybridization model. (b) a more general case.

In this work, we develop a new hybridization model for plasmons of strongly interacting many-particle systems. Our model combines the advantages of both the plasmon hybridization and TO approaches, thus providing a simple and intuitive picture when the particles are close-to-touching. More importantly, the proposed model leads to new physical insights into the relation between geometry and plasmons: how global and local features of the system's complex geometry affect the spectrum of the plasmons.

Before explaining our model, we mention that the non-local effect, which has a quantum origin, is an important issue when the gap distance is extremely small (below 0.5 nm) [61–66]. Our focus is *not* on modelling the non-local effect but on understanding the strong interaction between the particles. We shall assume the local model for the metal permittivity. The nonlocal effect can be accounted for by using the approach of [8, 63, 64].

We now explain our proposed model which we call the *Singular Hybridization (SH) Model*. In the standard hybridization model, a plasmon of the system is a combination of plasmons of individual particles. On the contrary, in our approach, the basic building blocks are the gap-plasmons of a pair of particles, and we use the TO approach to capture their singular behavior. This simple conceptual change is the key to solving the aforementioned challenges. In Figure 1a, we show a schematic comparison for a trimer, as it is the simplest example for our model (we emphasize that our model can be applied to a general configuration of particles as shown in Figure 1b). The trimer plasmon is now treated as a combination of two gap-plasmons. In our picture, the new plasmons are formed by the hybridization of these gap-plasmons. The gap-plasmons are strongly confined in their respective gaps and all the gaps are well-separated, which means that the gap-plasmons do not overlap significantly with each other. Hence, the spectral shifts due to their hybridization should be moderate. Therefore, we can expect that we still get a simple picture even in the close-to-touching case.

To gain a better understanding, we develop a coupled mode theory for the hybridization of singular gap-plasmons. For simplicity, we consider only 2D structures, however, our theory can be extended to the 3D case. We assume the Drude model for the metal permittivity $\epsilon = 1 - \frac{\omega_p^2}{\omega^2}$, where ω_p is the bulk plasma frequency and the background permittivity is $\epsilon_0 = 1$. We also adopt

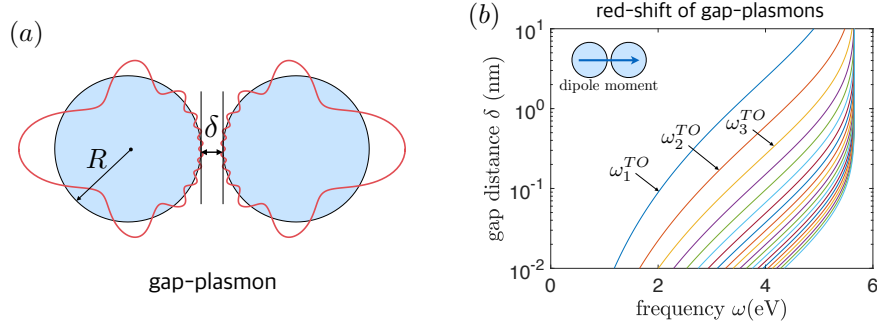


Figure 2: Gap-plasmon of a dimer. (A) oscillation of a gap-plasmon. (B) the red-shift of the spectrum. We set $R = 20$ nm and $\omega_p = 8$ eV.

the quasi-static approximation by assuming the system to be small compared to the wavelength of the incident light. We remark that the radiation reaction can be incorporated to go beyond the quasi-static limit, as described in [8].

We begin with the TO description [8,9] of gap-plasmons which are the basic building blocks of our proposed model. Consider a dimer of cylinders of radii R separated by a distance δ . TO has revealed that, when the two cylinders get closer, the wavelength of their plasmon near the gap becomes smaller and energy accumulation occurs in the gap region, which gives rise to an extreme field enhancement (Figure 2a). TO also can describe the singular spectral shift of gap-plasmons. Let us consider the gap-plasmons whose dipole moment is aligned parallel to the dimer axis since these plasmons contribute to the optical response significantly. Their resonance frequencies ω_n^{TO} are given by

$$\omega_n^{TO} = \omega_p \sqrt{e^{-ns} \sinh(ns)}, \quad n = 1, 2, 3, \dots,$$

with the parameter s satisfying $\sinh^2 s = (\delta/R)(1 + \delta/4R)$. We denote their associated gap-plasmons by $|\omega_n^{TO}\rangle$. When the gap distance δ gets smaller, as shown in Figure 2b, the frequencies ω_n^{TO} are red-shifted singularly and the spectrum becomes denser. Thus, the TO description captures the singular behavior of gap-plasmons.

We now turn to our model. We explain our model taking a trimer as an example (Figure 3a). The trimer plasmon is specified as a superposition of the gap-plasmon of the pair (B_1, B_2) and that of the pair (B_2, B_3) . We let (a_n, b_n) represent the following linear combination of the gap-plasmons: $a_n|\omega_n^{TO}(B_1, B_2)\rangle + b_n|\omega_n^{TO}(B_2, B_3)\rangle$. Their hybridization is characterized by the following coupled mode equations:

$$\begin{bmatrix} (\omega_n^{TO})^2 & \Delta_n \\ \Delta_n & (\omega_n^{TO})^2 \end{bmatrix} \begin{bmatrix} a_n \\ b_n \end{bmatrix} = \omega^2 \begin{bmatrix} a_n \\ b_n \end{bmatrix}.$$

Here, Δ_n represents the coupling between the two gap-plasmons. As the bonding angle θ between the two gap-plasmons decreases, the coupling strength Δ_n increases, which is to be expected since the two gaps get closer. This coupled mode system is derived using the spectral theory of the Neumann–Poincaré operator [67–69] and TO (see the supplementary materials for the details). We emphasize that the above equation is a simplified version of our theory. Although

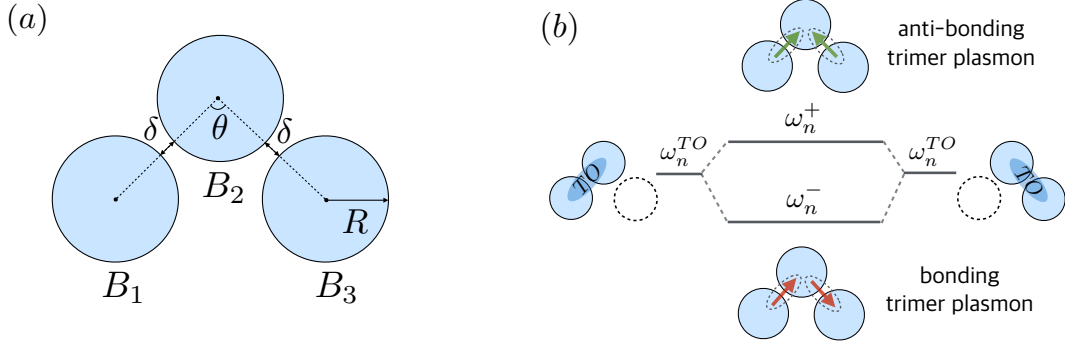


Figure 3: Trimer plasmons. (a) geometry of the trimer. The pairs (B_1, B_2) and (B_2, B_3) are close-to-touching while B_1 and B_3 are well-separated. (b) hybridization diagram.

we require additional TO gap-plasmons for improved accuracy, we shall see that this simplified version can already capture the physics. Solving the equation, we obtain the hybrid plasmons for the trimer

$$|\omega_n^\pm\rangle \approx \frac{1}{\sqrt{2}} \left(|\omega_n^{TO}(B_1, B_2)\rangle \mp |\omega_n^{TO}(B_2, B_3)\rangle \right), \quad n = 1, 2, 3, \dots,$$

and their resonance frequencies

$$\omega_n^\pm \approx \omega_n^{TO} \pm \Delta_n, \quad n = 1, 2, 3, \dots$$

So our theory predicts that the spectrum consists of a family of pairs (ω_n^-, ω_n^+) of resonance frequencies which are split from the dimer resonance frequencies ω_n^{TO} . The dimer part ω_n^{TO} is singularly shifted as the gap distance δ get smaller, while the splitting part Δ_n remains moderate. We call $|\omega_n^-\rangle$ and $|\omega_n^+\rangle$ the *bonding trimer plasmon* and *anti-bonding trimer plasmon*, respectively (Figure 3b). The bonding plasmon has a net dipole moment pointing in the x-direction so that it can be excited by the x-polarized light. Similarly, the anti-bonding plasmon can be excited by the y-polarized light. These plasmons are very different from the bonding plasmon and anti-bonding plasmon of a dimer in the standard hybridization model. They are trimer plasmons and are capable of capturing the close-to-touching interaction via TO. We also mention that in our model the physical picture for the trimer is quite different from the standard hybridization one given in [70].

We now discuss the physical implication of our SH model. The power of our model comes from its ability to decompose the spectrum into a singular part, which depends on the local geometry, and a regular part, which depends on the global geometry. The resonance frequency ω_n^\pm for the trimer consists of two parts: the singularly shifted part ω_n^{TO} and the regular splitting part Δ_n . The singular part ω_n^{TO} is determined by the small gap distance δ , which is a ‘local’ feature of the geometry. On the other hand, the regular part Δ_n is determined by the bonding angle θ , which is a ‘global’ feature of the geometry. In other words, the small gap distance δ affects the ‘overall’ behavior of the spectrum while the bonding angle θ controls the ‘detailed’ splitting

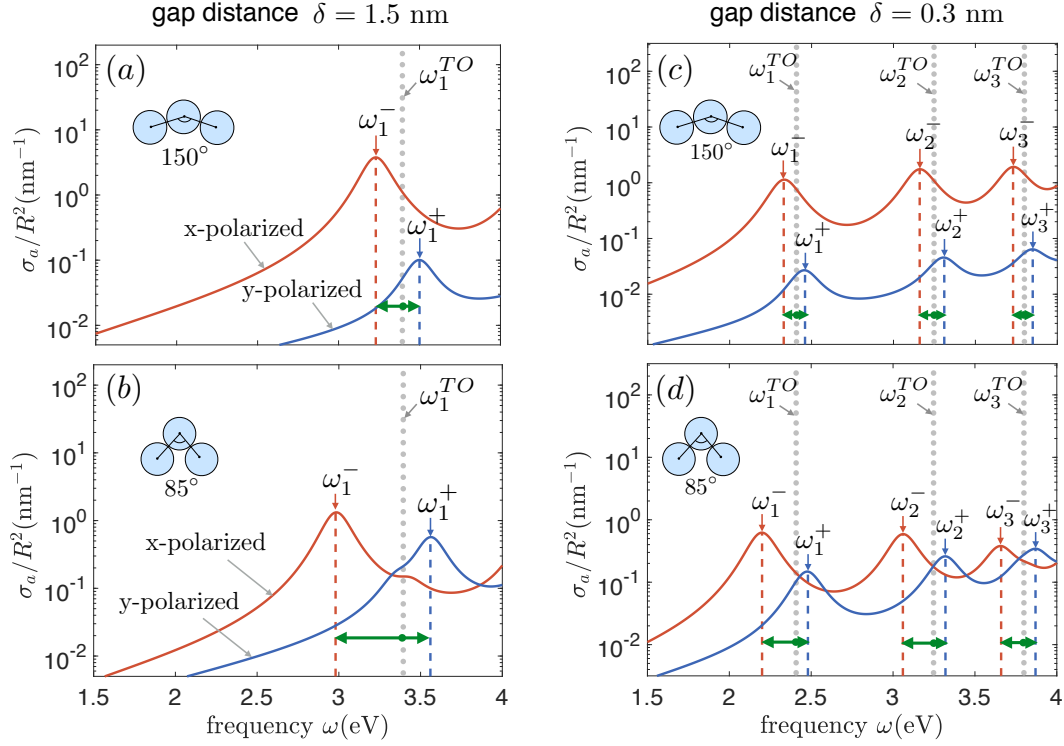


Figure 4: Absorption cross section σ_a for the trimer. (a, b) the gap distance $\delta = 1.5$ nm. (c, d) the gap distance $\delta = 0.3$ nm.

of the spectrum. This shows an interesting relation between the spectrum and the geometry: *local* (and *global*) features of the geometry can determine the *global* (and *local*) behavior of the spectrum, respectively. This relation provides us with a design principle: manipulation of the local geometrical singularity (such as inter-particle gap distances) to control the overall behavior of the spectrum, together with manipulation of the global geometry to achieve a detailed splittings of the spectrum. Our SH model provides a systematic way of achieving such a design using gap-plasmons as basic building blocks. We emphasize that our approach is valid for general systems consisting of an arbitrary number of interacting particles, with arbitrary positions and different radii, as long as the shape of each particle is circular in 2D or spherical in 3D.

We validate our model with numerical examples for the trimer. We set the radius of the particles to be $R = 30$ nm. We consider the two cases: when the inter-particle gap distance are (i) $\delta = 1.5$ nm and (ii) $\delta = 0.3$ nm. Notice that the ratio δ/R is very small so that the particles are nearly touching. We assume the Drude model $\epsilon = 1 - \omega_p^2/(\omega(\omega + i\gamma))$ with $\omega_p = 8$ eV and $\gamma = 0.2$ eV. In Figures 4a and 4b, we plot the absorption cross section for the trimer with the gap distance $\delta = 1.5$ nm when the bonding angle is $\theta = 150^\circ$ (weak coupling) and $\theta = 85^\circ$ (strong coupling), respectively. In the latter case, the coupling strength between the gap-plasmons is stronger since the gaps are closer to each other. The absorption cross section is computed by a 2D version of the numerical method developed in [60]. Similarly, in Figures 4c and 4d, we plot the absorption cross section in the case of the smaller gap distance $\delta = 0.3$

nm. We also plot the values of the resonance frequencies ω_n^- and ω_n^+ (red and blue dashed lines) computed by a complete version of our theory. Their corresponding plasmons are dominated by bonding and anti-bonding combinations of gap-plasmons, respectively. As expected, the resonance peaks of the absorption are located near the bonding (and anti-bonding) plasmon frequencies ω_n^- (and ω_n^+) for the x-polarized (and y-polarized) incident field, respectively. The gray dots represent the dimer frequency ω_n^{TO} computed using the TO approach. As the gap-distance δ gets smaller, the overall spectrum is significantly red-shifted in conjunction with the singular shift of ω_n^{TO} . The green arrows indicate how much the trimer frequencies ω_n^\pm have split from the dimer frequency ω_n^{TO} . The splitting $\omega_n^\pm - \omega_n^{TO}$ is clearly shown and it is moderate regardless of the inter-particle gap-distance. In the strong coupling case (smaller bonding angle), the splitting is more pronounced. Also, the absorption of the y-polarized incident field becomes stronger since the net dipole moment of the anti-bonding mode increases as the bonding angle θ decreases. Hence, the numerical results are consistent with the prediction of our proposed SH Model.

In conclusion, we have proposed the *Singular Hybridization Model* for plasmons of strongly interacting particles which gives a simple and intuitive physical picture when the particles are close-to-touching. The proposed model demonstrates an elegant interplay between the hybridization model and transformation optics, clarifying a deep geometrical dependence of the plasmon spectrum. We believe that our model can have a significant impact on the design of future plasmonic devices.

2 Supplementary Materials

Here we outline our coupled mode theory for the hybridization of singular gap-plasmons. We consider the 2D case for simplicity. We also assume the quasi-static approximation.

Integral equation approach for surface plasmons. Suppose we have a system of nanoparticles Ω with permittivity ϵ . We assume the background permittivity is $\epsilon_0 = 1$ and the electric field \mathbf{E}^{in} is incident. Then the induced charge density σ on the surfaces $\partial\Omega$ of the particles is determined by the following integral equation [67–69]

$$(\mathcal{K}_\Omega^* - \lambda I)[\sigma] = \mathbf{E}^{in} \cdot \mathbf{n}|_{\partial\Omega}, \quad \lambda = \frac{\epsilon + 1}{2(\epsilon - 1)},$$

where \mathcal{K}_Ω^* is the Neumann–Poincaré (NP) operator given by

$$\mathcal{K}_\Omega^*[\sigma](\mathbf{r}) = \frac{1}{2\pi} \int_{\partial\Omega} \frac{(\mathbf{r} - \mathbf{r}') \cdot \mathbf{n}(\mathbf{r})}{|\mathbf{r} - \mathbf{r}'|^2} \sigma(\mathbf{r}') dS(\mathbf{r}'), \quad \mathbf{r} \in \partial\Omega.$$

and \mathbf{n} is the outward unit normal vector to the surface. If the permittivity ϵ is negative, then the above problem may admit a solution even when the incident field \mathbf{E}^{in} is absent. In fact, this solution corresponds to the (localized) surface plasmon of the given system. More precisely, the mathematical analysis of the surface plasmons is equivalent to the following eigenvalue problem for the NP operator [67–69]:

$$\mathcal{K}_\Omega^*[\sigma] = \lambda\sigma, \quad \lambda = \frac{\epsilon + 1}{2(\epsilon - 1)}.$$

If we model the metal permittivity by Drude's model in which $\epsilon = 1 - \omega_p^2/\omega^2$, then the above eigenvalue problem can be rewritten as

$$\mathcal{A}_\Omega[\sigma] := \omega_p^2 \left(\frac{1}{2} I - \mathcal{K}_\Omega^* \right) [\sigma] = \omega^2 \sigma.$$

Let ω_n^2 and σ_n be the eigenvalues and eigenfunctions of the operator \mathcal{A}_Ω . Then ω_n (and σ_n) represents the resonance frequency (and the charge density) of plasmons, respectively. Let us denote the plasmon charge density σ_n by $|\omega_n\rangle$ to indicate that its resonance frequency is ω_n .

Let us define an inner product $\langle \omega_n | \omega_{n'} \rangle$ of two plasmons $|\omega_n\rangle$ and $|\omega_{n'}\rangle$ by

$$\langle \omega_n | \omega_{n'} \rangle = \int_{\partial\Omega} \sigma_n(\mathbf{r}) \int_{\partial\Omega} \frac{(-1)}{2\pi} \log |\mathbf{r} - \mathbf{r}'| \sigma_{n'}(\mathbf{r}') dS(\mathbf{r}') dS(\mathbf{r}).$$

It can be shown that the eigenfunctions of the operator \mathcal{K}_Ω^* (hence \mathcal{A}_Ω) form a complete orthogonal basis with respect to the above inner product.

TO description of the dimer plasmons. Consider the dimer $D = B_+ \cup B_-$ where B_\pm is a circular cylinder of radius R centered at $\pm(R + \delta/2, 0)$. Note that the two particles B_+ and B_- are separated by a distance δ . Using the TO approach [8,9], we can derive the dimer plasmons (*i.e.* the eigenvalues and eigenfunctions of the operator \mathcal{A}_D) explicitly. The conformal transformation Φ given by

$$x' + iy' = \Phi(x + iy) = \frac{x + iy + a}{x + iy - a}, \quad a = (\delta(R + \delta/4))^{1/2},$$

maps the dimer to a concentric annulus whose inner radius is $r_i = e^{-s}$ and outer radius is $r_e = e^s$, where $\sinh s = a/R$. Let (r', θ') be the polar coordinates of the transformed frame, namely, $z' = x' + iy' = r' e^{i\theta'}$. As mentioned in the manuscript, we consider only the dimer plasmons whose dipole moment is aligned in the x -direction. The resonance frequencies of these plasmons are

$$\omega_n^{TO} = \omega_p \sqrt{e^{-ns} \sinh(ns)}, \quad n = 1, 2, 3, \dots,$$

and their associated plasmon charge densities $|\omega_n^{TO}\rangle$ are given as follows: for $n = 1, 2, 3, \dots$,

$$|\omega_n^{TO}\rangle(\mathbf{r}) = \pm \frac{1}{\sqrt{N_n}} \frac{\cosh s - \cos \theta'}{\alpha} \cos n\theta', \quad \mathbf{r} \in \partial B_\pm,$$

where the normalization constant N_n is chosen such that $\langle \omega_n^{TO} | \omega_n^{TO} \rangle = 1$. We can verify that $|\omega_n^{TO}\rangle$ are the eigenfunctions of \mathcal{A}_D with the eigenvalues $(\omega_n^{TO})^2$, namely, $\mathcal{A}_D |\omega_n^{TO}\rangle = (\omega_n^{TO})^2 |\omega_n^{TO}\rangle$.

Hybridization of singular plasmons: a trimer case. Next, we consider the trimer $T = B_1 \cup B_2 \cup B_3$ given in the manuscript. Recall that the pairs (B_1, B_2) and (B_2, B_3) are close-to-touching while B_1 and B_3 are well-separated. After some translation and rotation and by abuse of notation, we can define the TO dimer plasmons for the pair (B_1, B_2) and the pair (B_2, B_3)

as follows:

$$|\omega_n^{TO}(B_1, B_2)\rangle = \begin{cases} |\omega_n^{TO}\rangle & \text{on } \partial B_1 \cup \partial B_2, \\ 0 & \text{on } \partial B_3, \end{cases}$$

and

$$|\omega_n^{TO}(B_2, B_3)\rangle = \begin{cases} 0 & \text{on } \partial B_1, \\ |\omega_n^{TO}\rangle & \text{on } \partial B_2 \cup \partial B_3. \end{cases}$$

These two dimer plasmons hybridize to form new modes. We approximate a hybridized mode $|\omega_n\rangle$ as a linear combination $|\omega_n\rangle = a_n|\omega_n^{TO}(B_1, B_2)\rangle + b_n|\omega_n^{TO}(B_2, B_3)\rangle$. This is a good approximation when the gap distance δ is small. In fact, we can prove that the set of $|\omega_n^{TO}(B_i, B_j)\rangle$ form an 'almost' orthogonal basis. More precisely, as $\delta \rightarrow 0$,

$$\langle \omega_n^{TO}(B_1, B_2) | \omega_{n'}^{TO}(B_2, B_3) \rangle \approx 0 \quad \text{for all } n, n' = 1, 2, 3, \dots,$$

and consequently,

$$\langle \omega_n | \omega_{n'} \rangle \approx 0 \quad \text{for } n \neq n'.$$

Using the fact that $\mathcal{A}_D|\omega_n^{TO}\rangle = (\omega_n^{TO})^2|\omega_n^{TO}\rangle$, we can easily see that

$$\begin{bmatrix} (\omega_n^{TO})^2 & \Delta_n \\ \Delta_n & (\omega_n^{TO})^2 \end{bmatrix} \begin{bmatrix} a_n \\ b_n \end{bmatrix} = \omega^2 \begin{bmatrix} a_n \\ b_n \end{bmatrix},$$

where Δ_n is given by

$$\Delta_n = \langle \omega_n^{TO}(B_1, B_2) | \mathcal{A}_T | \omega_n^{TO}(B_2, B_3) \rangle.$$

By finding the eigenvalues and eigenvectors of the matrix on the LHS, we can find good approximations for the hybrid plasmons and their resonance frequencies. The interaction term Δ_n can be computed analytically using the connection between TO and the method of image charges [60]. By including a full set of basis (the gap-plasmons with different TO angular momenta n and the gap-plasmons for the other pair (B_1, B_3)), we can compute all the resonance frequencies and their associated plasmon modes accurately. We remark that this model is also numerically efficient in the nearly touching case. As mentioned in the main text, it is straightforward to extend the above coupled mode theory to a more general system of particles.

References

- [1] E. Ozbay, Plasmonics: merging photonics and electronics at nanoscale dimensions. *Science* 311, 189-193 (2006).
- [2] S. Lal, S. Link and N. J. Halas, Nano-optics from sensing to waveguiding. *Nat. Photon.* 1, 641648 (2007)
- [3] J. A. Schuller et al., Plasmonics for extreme light concentration and manipulation. *Nat. Mat.* 9, 193 (2010).

- [4] B. Luk'yanchuk et al., The Fano resonance in plasmonic nanostructures and metamaterials. *Nat. Mat.* 9, 707 (2010).
- [5] N. J. Halas, S. Lai, W-S Chang, S. Link and P. Nordlander, Plasmons in strongly coupled metallic nanostructures. *Chem. Rev.* 111, 3913–3961 (2011).
- [6] E. Prodan, C. Radloff, N. J. Halas, P. Nordlander, A hybridization model for the plasmon response of complex nanostructures. *Science* 302, 419–422 (2003).
- [7] P. Nordlander, C. Oubre, E. Prodan, K. Li and M. I. Stockman, Plasmon hybridization in nanoparticle dimers. *Nano Lett.* 4, 899–903 (2004).
- [8] J. B. Pendry, A. Aubry, D. R. Smith and S. A. Maier, Transformation optics and subwavelength control of light. *Science*, 337 (2012), pp. 549–552.
- [9] J. B. Pendry, Y. Luo and R. Zhao, Transforming the optical landscape. *Science* 348, 521–524 (2015).
- [10] J. B. Pendry, A. I. Fernandez-Domnguez, Y. Luo and R. Zhao, Capturing photons with transformation optics. *Nat. Phys.*, 9 (2013), pp. 518–522.
- [11] H. Ammari, H. Kang and M. Lim, Gradient estimates for solutions to the conductivity problem, *Math. Ann.* 332(2) (2005), 277286.
- [12] H. Ammari, H. Kang, H. Lee, J. Lee, and M. Lim, Optimal estimates for the electric field in two dimensions, *J. Math. Pures Appl.*, 88 (2007), pp. 307-324.
- [13] H. Ammari, H. Kang, H. Lee, M. Lim and H. Zribi, Decomposition theorems and fine estimates for electrical fields in the presence of closely located circular inclusions, *J. Differ. Equations* 247 (2009), 2897-2912.
- [14] H. Ammari, G. Ciruolo, H. Kang, H. Lee, and K. Yun, Spectral analysis of the Neuman-Poincaré operator and characterization of the stress concentration in anti-plane elasticity *Arch. Ration. Mech. Anal.* 208, 275–304 (2013).
- [15] E. S. Bao, Y. Y. Li, and B. Yin, Gradient estimates for the perfect conductivity problem, *Arch. Rational Mech. Anal.*, 193 (2009), pp. 195-226.
- [16] J. Bao, H. Li, and Y. Li, Gradient estimates for solutions of the Lamé system with partially infinite coefficients, *Arch. Rational Mech. Anal.*, 215 (2015), pp. 307-351.
- [17] J. Bao, H. Li, and Y. Li, Gradient estimates for solutions of the Lamé system with partially infinite coefficients in dimensions greater than two, *Adv. Math.* 305 (2017), 298-338.
- [18] E. Bonnetier, and F. Triki, *AMS Contemporary Math.* 577, 81–92 (2012).
- [19] E. Bonnetier and F. Triki, On the spectrum of the Poincar variational problem for two close-to-touching inclusions in 2D. *Arch. Ration. Mech. Anal.* 209, 541–567 (2013).
- [20] D. J. Bergman, The dielectric constant of a simple cubic array of identical spheres, *J. Phys. C: Solid State Phys.* 12 (1979) 4947.

- [21] I. Babuska, B. Andersson, P. Smith and K. Levin, Damage analysis of fiber composites. I. Statistical analysis on fiber scale, *Comput. Methods Appl. Mech. Engrg.* 172 (1999), 2777.
- [22] L. Berlyand and A. Kolpakov, Network approximation in the limit of small interparticle distance of the effective properties of a high-contrast random dispersed composite, *Arch. Rational Mech. Anal.* 159 (2001), 179-227.
- [23] L. Berlyand, L. Borcea and A. Panchenko, Network approximation for effective viscosity of concentrated suspensions with complex geometry. *SIAM J. Math. Anal.* 36 (2005), 1580-1628.
- [24] L. Berlyand, A. G. Kolpakov and A. Novikov. *Introduction to the network approximation method for materials modeling* (Cambridge University Press, 2013).
- [25] L. Borcea, Y. Gorb and Y. Wang, Asymptotic approximation of the Dirichlet to Neumann Map of high contrast conductive media, *Multiscale Model. Simul.* 12 (2014) 14941532.
- [26] Y. Gorb, Singular behavior of electric field of high contrast concentrated composites, *SIAM Multiscale Model. Simul.* 13 (2015), 1312-1326.
- [27] Y. Gorb and A. Novikov, Blow-up of solutions to a p-Laplace equation, *SIAM Multiscale Model. Simul.* 10 (2012), 727743.
- [28] J. B. Keller, Conductivity of a medium containing a dense array of perfectly conducting spheres or cylinders or nonconducting cylinders, *J. Appl. Phys.* 34 (1963), 991993.
- [29] H. Kang, H. Lee, and K. Yun, Optimal estimates and asymptotics for the stress concentration between closely located stiff inclusions, *Math. Ann.*, 363 (2015), pp. 1281-1306.
- [30] H. Kang and S. Yu, A proof of the Flaherty-Keller formula on the effective property of densely packed elastic composites, *arXiv:1707.02205*.
- [31] H. Kang and S. Yu, Quantitative characterization of stress concentration in the presence of closely spaced hard inclusions in two-dimensional linear elasticity, *arXiv:1707.02207*.
- [32] H. Kang and K. Yun, Optimal estimates of the field enhancement in presence of a bowtie structure of perfectly conducting inclusions in two dimensions, *arXiv:1707.00098*.
- [33] J. Kim and M. Lim, Electric field concentration in the presence of an inclusion with eccentric core-shell geometry, *Math. Ann.* (2018). <https://doi.org/10.1007/s00208-018-1688-6>
- [34] M. Lim and K. Yun, Blow-up of electric fields between closely spaced spherical perfect conductors, *Commun. Part. Diff. Eq.* 34, 1287-1315 (2009).
- [35] M. Lim and K. Yun, Strong influence of a small fiber on shear stress in fiber-reinforced composites, *J. Differ. Equations* 250 (2011), 24022439.
- [36] M. Lim and S. Yu, Asymptotics of the solution to the conductivity equation in the presence of adjacent circular inclusions with finite conductivities. *J. Math. Anal. Appl.* 421, 131–156 (2015).

- [37] Y. Li and L. Nirenberg, Estimates for elliptic systems from composite material, *Comm. Pure Appl. Math.* 56 (2003), 892-925.
- [38] Y. Li and M. Vogelius, Gradient estimates for solutions of divergence form elliptic equations with discontinuous coefficients, *Arch. Rat. Mech. Anal.* 153 (2000), 91-151.
- [39] J. Lekner, Near approach of two conducting spheres: Enhancement of external electric field, *J. Electrostatics*, 69 (2011), pp. 559-563.
- [40] J. Lekner, Electrostatics of two charged conducting spheres, *Proc. R. Soc. A*, 468 (2012), pp. 2829-2848.
- [41] R. C. McPhedran and D. R. McKenzie, Electrostatic and optical resonances of arrays of cylinders, *Appl. Phys.* 23 (1980), 223-235.
- [42] R. C. McPhedran and W. T. Perrins, Electrostatic and optical resonances of cylinder pairs. *Appl. Phys. A* 24 (1981) 311-318.
- [43] R. C. McPhedran and G. W. Milton, Transport properties of touching cylinder pairs and of the square array of touching cylinders, *Proc. R. Soc. A*, 411 (1987), pp. 313-326.
- [44] R. C. McPhedran, L. Poladian and G. W. Milton, Asymptotic studies of closely spaced, highly conducting cylinders, *Proc. R. Soc. A*, 415 (1988), pp. 185-196.
- [45] G. W. Milton, *The Theory of Composites* (Cambridge University Press, 2002).
- [46] V. Mityushev and N. Rylko, A fast algorithm for computing the flux around non-overlapping disks on the plane, *Math. Comput. Model.* 57 (2013) 1350-1359.
- [47] V. Mityushev, Pattern formations and optimal packing, *Math. Biosciences* 274 (2016) 12-16.
- [48] V. Mityushev, Optimal and stable random pattern formations, *Jour. Theo. Bio.* 422 (2017) 1217.
- [49] L. Poladian, General theory of electrical images in sphere pairs, *Quart. J. Mech. Appl. Math.*, 41 (1988), pp. 395-417.
- [50] L. Poladian, Asymptotic behaviour of the effective dielectric constants of composite materials, *Proc. R. Soc. A*, 426 (1989), pp. 343-359.
- [51] L. Poladian, thesis, University of Sydney (1990).
- [52] N. Rylko, Structure of the scalar field around unidirectional circular cylinders, *Proc. R. Soc. A* (2008) 464, 391-407.
- [53] N. Rylko, A pair of perfectly conducting disks in an external field, *Math. Model. and Anal.* 20 (2015), 273-288.
- [54] O. Schnitzer, Singular perturbations approach to localized surface-plasmon resonance: Nearly touching metal nanospheres. *Phys. Rev. B* 92, 235428 (2015).

- [55] O. Schnitzer, V. Giannini, S. A. Maier and R. V. Craster, Surface plasmon resonances of arbitrarily shaped nanometallic structures in the small-screening-length limit. *Proc. R. Soc. A* 472, 20160258 (2016).
- [56] O. Schnitzer, Asymptotic approximations for the plasmon resonances of nearly touching spheres. *arXiv:1807.01636* (2018).
- [57] A. L. Vanel, O. Schnitzer and R. V. Craster, Asymptotic network models of subwavelength metamaterials formed by closely packed photonic and phononic crystals, *EPL (Europhysics Letters)* 119 (2017), 64002.
- [58] K. Yun, Estimates for electric fields blown up between closely adjacent conductors with arbitrary shape, *SIAM J. Appl. Math.*, 67 (2007), pp. 714-730.
- [59] K. Yun, An optimal estimate for electric fields on the shortest line segment between two spherical insulators in three dimensions, *J. Differential Equations*, 261 (2016), pp. 148-188.
- [60] S. Yu and H. Ammari, Plasmonic interaction between nanospheres. *SIAM Rev.* 60, 356–385 (2018).
- [61] J. Zuloaga, E. Prodan and P. Nordlander, Quantum description of the plasmon resonances of a nanoparticle dimer. *Nano Lett.* 9, 887-891 (2009).
- [62] C. Ciracì et al., Probing the ultimate limits of plasmonic enhancement. *Science* 337, 1072–1074 (2012).
- [63] Y. Luo, A. I. Fernandez-Dominguez, A. Wiener, S. A. Maier and J. B. Pendry, Surface plasmons and nonlocality: a simple model. *Phys. Rev. Lett.* 111, 093901 (2013).
- [64] Y. Luo, R. Zhao, and J. B. Pendry, van der Waals interactions at the nanoscale: The effects of nonlocality. *Proc. Nat. Acad. Sci. U.S.A.* 111, 18422–18427 (2014).
- [65] W. Zhu et al., Quantum mechanical effects in plasmonic structures with subnanometre gaps. *Nat. Commun.* 7, 11495 (2016).
- [66] O. Schnitzer, V. Giannini, R. V. Craster and S. A. Maier, Asymptotics of surface-plasmon redshift saturation at subnanometric separations, *Phys. Rev. B* 93, 041409 (2016).
- [67] I. D. Mayergoyz et al., Electrostatic (plasmon) resonances in nanoparticles. *Phys. Rev. B* 72, 155412 (2005).
- [68] K. Ando, H. Kang, Analysis of plasmon resonance on smooth domains using spectral properties of the Neumann-Poincaré operators. *J. Math. Anal. Appl.* 435, 162–178 (2016).
- [69] H. Ammari, Y. Deng and P. Millien, Surface plasmon resonance of nanoparticles and applications in imaging. *Arch. Ration. Mech. Anal.* 220, 109–153 (2016).
- [70] D. W. Brandl, N. A. Mirkin and P. Nordlander, Plasmon modes of nanosphere trimers and quadrumers. *J. Phys. Chem. B* 110, 12302-12310 (2006).